REKAYASA
Journal of Science and Technology
https://journal.trunojoyo.ac.id/rekayasa

Rekayasa, 2025; 18(1): 83-94
ISSN: 0216-9495 (Print)
ISSN: 2502-5325 (Online)

# Modeling of Conventional Single Slope Solar Still (CS4) with Phase Change Material (PCM)

Irfan Santosa[1*], Muhamad Dwi Septiyanto[1], Sholikhin Andriyanto[1], Eko Prasetya Budiana[1] Syamsul Hadi[1] Agung Tri Wijayanta[1]
[1] Department of Mechanical Engineering Faculty of Engineering Universitas Sebelas Maret
Jl Ir Sutami 36A Surakarta 57126 Central Java Indonesia
*E-mail Korespondensi : ubaidillah.ms@trunojoyo.ac.id
DOI: https://doi.org/10.21107/rekayasa.v18i1.28173
Submitted November 25th 2024, Accepted April 3rd 2025, Published April 30th 2025

***Abstrak***

Studi ini menyelidiki kemampuan simulasi CFD (Computational Fluid Dynamics) dua dimensi untuk memperkirakan pola distribusi suhu dan kontur kecepatan pada alat penyuling surya lereng tunggal yang menggunakan material soybean wax sebagai pengubah fase (PCM). Jenis mesh yang digunakan model segitiga. Geometri basin menggunakan jumlah mesh 20402 nodes, 10000 elemen dan geometri PCM menggunakan jumlah mesh 9272 nodes, 4500 elemen. Studi ini memperkenalkan persamaan yang dikembangkan berdasarkan analogi Dunkle, Bulk Motion, dan Chilton-Colburn, untuk memperkirakan nilai Nusselt pada alat penyuling surya. Suhu air (Tw), suhu permukaan dalam penutup kaca (Tg), dan suhu PCM (Tpcm) ditentukan melalui pengujian eksperimental, sedangkan kinerja sistem distilasi surya konvensional diprediksi berdasarkan hasil eksperimen dengan teori. Hasil penelitian menunjukkan bahwa penggunaan lilin kedelai sebagai PCM memberikan pengaruh positif terhadap distribusi suhu dan pola garis arus dalam alat penyuling surya lereng tunggal. Pada pagi hari, distribusi temperatur dan kecepatan menunjukkan bahwa garis isoterm sejajar dengan segmen kanan bawah rongga, yang mengindikasikan bahwa konveksi mulai terbentuk dalam pola aliran ini. Semakin siang, pola streamline pada rongga menjadi besar melengkung, yang menunjukkan peningkatan dalam proses konveksi. Temuan ini konsisten dengan hasil analisis CFD, yang mempunyai akurasi tinggi dalam memprediksi nilai Nusselt. Selain itu, perbandingan antara produktivitas air suling harian dari data eksperimen dan hasil teori menunjukkan kesesuaian yang baik.
**Kata Kunci:** simulasi CFD, penyuling surya, pengubah fase, nilai Nusselt

***Abstract***

*This study investigates the capability of two-dimensional Computational Fluid Dynamics (CFD) simulation to estimate the temperature distribution pattern and velocity contours in a single slope solar still that uses soybean wax as a phase change material (PCM). A triangular mesh model is employed in the simulation. The basin geometry uses a mesh with 20,402 nodes and 10,000 elements, while the PCM geometry uses a mesh consisting of 9,272 nodes and 4,500 elements. This study introduces an equation developed based on the Dunkle, Bulk Motion, and Chilton-Colburn analogies to estimate the Nusselt number in the solar still. The water temperature (Tw), the inner surface temperature of the glass cover (Tg), and the PCM temperature (Tpcm) are determined experimentally, whereas the performance of the conventional solar distillation system is predicted theoretically using the experimental results. The results demonstrate that the use of soybean wax as a PCM positively influences the temperature distribution and streamline patterns within the single slope solar still. In the morning, the temperature and velocity distributions reveal that the isotherm lines are parallel to the lower right segment of the cavity, indicating that a convection flow pattern is beginning to form. As the day progresses, the streamline pattern inside the cavity expands and becomes more curved, suggesting an increased influence of the convection process. These findings are consistent with the CFD analysis results, which show high accuracy in predicting Nusselt numbers. Furthermore, the comparison between daily distilled water productivity from experimental measurements and theoretical predictions shows good agreement.*

***Key words**: CFD simulation, solar still, phase change, Nusselt numbers*

## INTRODUCTION

The growing demand for water due to irrigation and human activities is driving global efforts to find alternative methods for producing distilled water, particularly from seawater. In this context, using solar distillers rather than traditional distillation methods effectively protects the environment and minimizes fuel consumption (Kabeel & El-Said, 2015). The single-slope solar still (S4) is a straightforward device configuration that harnesses solar energy for the desalination process, producing distilled water from brine (Bansal et al., 2022). Additionally, solar radiation is offered on-site, free, and never-ending. The assessment of solar still performance can be broadly divided into two types of research: theoretical and experimental. Much of the experimental research is to build up different kinds of solar stills or enhance their production and functionality. Rajaseenivasan & Srithar (2016), utilized square and hollow circular fins to enhance the productivity and efficiency of the single-slope solar still. A study was conducted to test the single-slope solar still using hollow circular fins (0.03 m dia x 0.07 m height) and square hollow (0.019 m side length x 0.07 m height) as absorbers, and the efficiency is 36%, and 45.8%. The other research showed a 45.5% increase in distilled water productivity when fins were used at the bottom of the still (Velmurugan et al., 2008). The experimental analysis of vertical and inclined circular fin as the variation was researched by (Ghougali et al., 2024), and the results efficiency gains of 33.84%, and 48.94%. In addition, many experimental studies have been conducted regarding phase change materials (PCM) affecting the performance of single-slope solar stills.

Saad et al. (2024) studied experimentally the effect of using phase change materials (PCM) melting temperature on improving single slope solar still productivity. They discovered that using 1.8 kg of PCM could boost total production by 124.74% and 51.91% for soy wax, by 110.68% and 45.72% for vaseline, and by 103.18% and 43.35% for paraffin during spring and summer, respectively. Jahanpanah et al. (Jahanpanah et al., 2021) conducted experimental research on the impact of Phase Change Materials (PCM) on the performance of single-slope solar still. They observed that incorporating PCM improved the solar still's efficiency from 28.13% to 36.42%. Singh et al. (2024), the research results from the overall thermal efficiencies are 26.64%, 29.09%, 31.58%, 22.03%, 24.63%, and 27.12% for the PCM materials (Paraffin wax, $MgCl_2.6H_2O$, KCl) and nano additives ($TiO_2$ and CuO), respectively. Shalaby et al. (Shalaby et al., 2016) investigated a new design of a v-corrugated absorber solar still with built-in phase change material (PCM). The results show that water productivity is maximum with PCM and corrugated plates used, even with lower water feed. Additionally, they concluded that employing PCM extends water production into the night and lowers the cost per unit of fresh water produced.

In recent years, researchers have focused on studying the effects of incorporating PCM into the operation of solar stills through numerical and theoretical methods. Alwan (Alwan et al., 2022), research on the performance solar still theoretically and experimentally. The same trend shows distribution and productivity yielded good results with errors of approximately 4.7% deviation. Clark (1990) introduced a new experimental model with extended operating ranges. They observed that under steady-state conditions, the constant in their model was half that of Dunkle's model, attributable to equal rates of evaporation and condensation. The productivity improvement of single-slope solar still using phase-changing material will be analyzed using Computational Fluid Dynamics (CFD). The results of the experiment and CFD analysis validate the consistency of the findings (Gnanavel et al., 2021). Prakash et al., (2022), investigated the temperature distribution in a single-slope solar still using CFD. The results of this research utilize CFD to develop a mathematical model that can be used to predict flow parameters and solve differential energy balance equations, which can be applied to solar distillation equipment to support researchers, scientists, and academics. Sarhaddi et al., (2017) performed a numerical comparison of cascade solar stills with and without PCM. They validated their results against experimental data and found that incorporating PCM significantly enhances both energy and exergy performance. Cheng et al. (2019) conducted both numerical and experimental studies on single slope solar still featuring a newly designed shape with stabilized PCM. Their numerical results indicated that the use of PCM could boost productivity by up to 53% compared to a conventional solar still. Taylor et al., (2012) investigate the natural convection effect in a 2-D single-slope solar still and find that the region where the flow moves downward from glass to water exhibits the highest heat transfer coefficient. El-Sebaii et al. (2009) investigated a transient mathematical model of single-slope solar still with and without a stearic acid PCM unit. As a result, the evaporative heat transfer coefficient is increased by 27% on using 3.3 cm of stearic acid as PCM.

From the comprehensive literature review presented above, it can be concluded that most research on the impact of PCM soybean wax on solar still performance has been either experimental or theoretical, with significantly fewer CFD analyses. Based on experimental data, this study aims to fill this gap by thoroughly investigating natural convection, including temperature and streamlined contours, in a single-slope solar still that uses PCM soybean wax for heat storage. It will also evaluate how closely theoretical predictions match with experimental results concerning distilled water productivity.

## RESEARCH METHOD

### Computational modeling

The modeling of a single-slope solar still with PCM using Fluent software (license number 1142698) will be investigated. The 2D geometry of the single-slope solar still is as follows: it has a width of 60 cm, a height of 40 cm on the right side, and 18 cm on the left side, and the glass cover is inclined at $26^0$. The bottom of the solar still is lined with soybean wax PCM with a thickness of 6 cm. The geometry of the single-slope solar still with PCM and the computational grid (20402 nodes, 10000 elements for the basin, and 9272 nodes, 4500 elements for the PCM) is depicted in Figure 1. Figure 2 illustrates the steps involved in CFD analysis. The profile temperature water (*Tw*), inner glass cover (*Tg*), and PCM (*Tpcm*) are based on experiments in our group research (Sadewa et al., 2024) as shown in Figure 3. The remaining boundary conditions include insulated side walls, no-slip momentum conditions, and zero species gradients. The lower cavity wall separates the air-$H_2O$ from the PCM-soybean wax, which is kept at a high temperature (TH) and high concentration (cH). The air-$H_2O$ mixture in the cavity is assumed to be incompressible and to flow smoothly. The liquid PCM soybean wax is also considered an incompressible and Newtonian fluid. The continuity, momentum, energy, and concentration equations are solved within the domain. Humid air is treated as an ideal gas, and Table 1 presents the thermophysical properties of soybean wax, while data for the air-$H_2O$ mixture are shown in Table 2. The governing equations used : (Saleem et al., 2020)

1. Continuity equation
$$\frac{\partial U}{\partial X} + \frac{\partial V}{\partial Y} = 0 \tag{1}$$
2. Momentum –x equation
$$U\frac{\partial U}{\partial X} + V\frac{\partial U}{\partial Y} = -\frac{1}{\rho}\frac{\partial P}{\partial X} + \mu\left(\frac{\partial^2 U}{\partial X^2} + \frac{\partial^2 U}{\partial Y^2}\right) \tag{2}$$
3. Momentum –y equation
$$U\frac{\partial V}{\partial X} + V\frac{\partial V}{\partial Y} = -\frac{1}{\rho}\frac{\partial P}{\partial X} + \mu\left(\frac{\partial^2 V}{\partial X^2} + \frac{\partial^2 V}{\partial Y^2}\right) \tag{3}$$
4. Energy equation
$$U\frac{\partial T}{\partial X} + V\frac{\partial T}{\partial Y} = \alpha\left(\frac{\partial^2 T}{\partial X^2} + \frac{\partial^2 T}{\partial Y^2}\right) \tag{4}$$
5. Concentration equation
$$U\frac{\partial C}{\partial X} + V\frac{\partial C}{\partial Y} = D\left(\frac{\partial^2 C}{\partial X^2} + \frac{\partial^2 C}{\partial Y^2}\right) \tag{5}$$

Table 1. *Properties soybean wax.*

| ***Properties*** | ***Soybean wax*** |
|---|---|
| Melting temperature ($^0$C) | 43.9 (Trisnadewi et al., 2021) |
| Latent heat (kJ/kg) | 100.90 (Yoo et al., 2019) |
| Thermal conductivity(W/m K) | 0.25 (Jeon et al., 2019) |
| Density (Kg/m$^3$) | 900 (Jeon et al., 2019) |
| Specific heat capacity (kJ/Kg K) | 0.496 (Jeon et al., 2019) |

Table 2. Thermophysical properties of air-H2O mixture (Saleem et al., 2020)

| ***Properties*** | ***Air-$H_2O$ mixture*** |
|---|---|
| Density (kg m$^{-3}$) | 1.11 |
| Specific heat (J kg$^{-1}$ K$^{-1}$) | 1.01 x $10^3$ |
| Thermal conductivity (W/m K) | 2.74 x $10^{-2}$ |
| Viscocity (kg m$^{-1}$ s$^{-1}$) | 1.92 x $10^{-5}$ |
| Diffusion coeficient (m$^2$ s$^{-1}$) | 2.82 x $10^{-5}$ |

Table 3. Boundary and initials conditions ) the depicted dimensional boundary conditions for Eqs. (1) - (5) (Saleem et al., 2021)

| **Air-$H_2O$ mixture** | | | |
|---|---|---|---|
| Floor | $T = T_h$ | $C = C_h$ | $U = V = 0$ |
| Oblique wall | $-k_\infty \frac{\partial T}{\partial n} = h_\infty (T - T_\infty)$ | $C = C_1$ | $U = V = 0$ |
| Left wall | $\frac{\partial T}{\partial X} = 0$ | $\frac{\partial c}{\partial x} = 0$ | $U = V = 0$ |
| Right wall | $\frac{\partial T}{\partial X} = 0$ | $\frac{\partial c}{\partial x} = 0$ | $U = V = 0$ |

| **PCM Soybean wax** | | | |
|---|---|---|---|
| Top wall | $T = T_h$ | – | $\dot{U} = \dot{V} = 0$ |
| Bottom wall | $\frac{\partial T}{\partial X} = 0$ | – | $\dot{U} = \dot{V} = 0$ |
| Left wall | $\frac{\partial T}{\partial X} = 0$ | – | $\dot{U} = \dot{V} = 0$ |
| Right wall | $\frac{\partial T}{\partial X} = 0$ | – | $\dot{U} = \dot{V} = 0$ |

The equations described above were solved using the finite volume method on a staggered grid. The SIMPLEC algorithm was employed to solve the steady fluid flow, heat, and mass transfer equations. The second-order upwind scheme was applied to solve the energy and water species equations. An implicit iterative method with successive under-relaxation was used to determine all variables at each node during each time step.

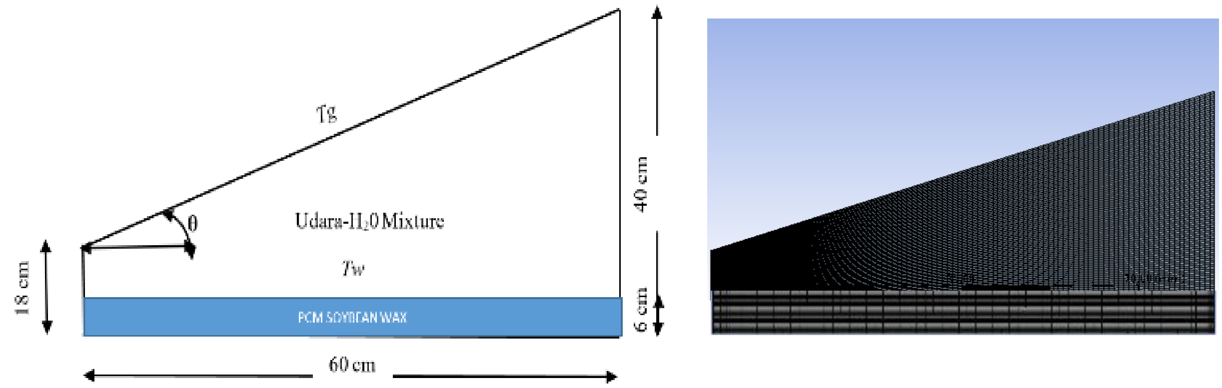


Figure 1. Geometry and mesh of a single slope solar still with PCM

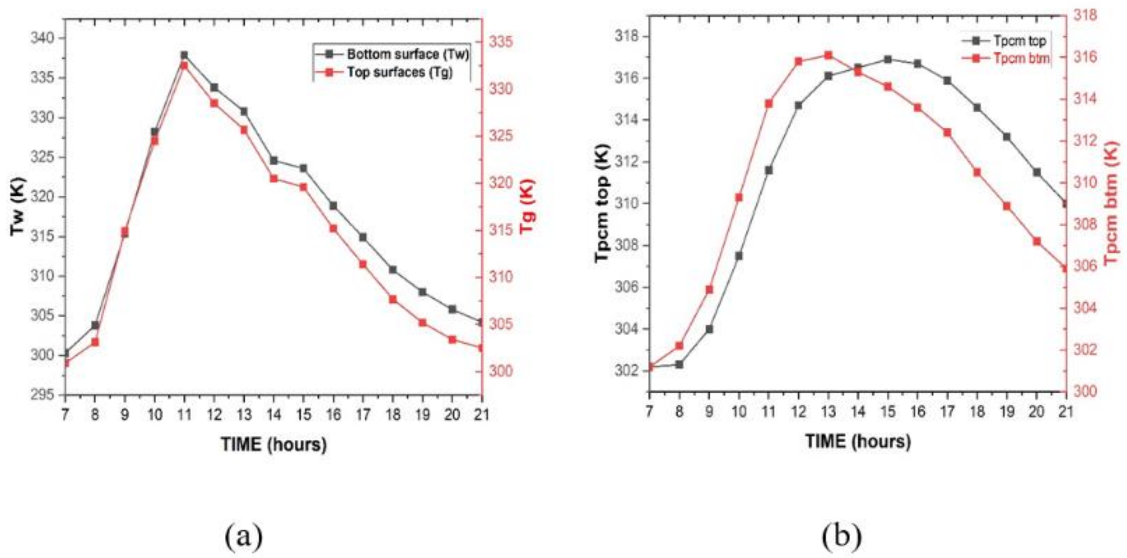


Figure 2. Specified temperature boundary conditions (a) internal basin, and (b) PCM temperature by experiments

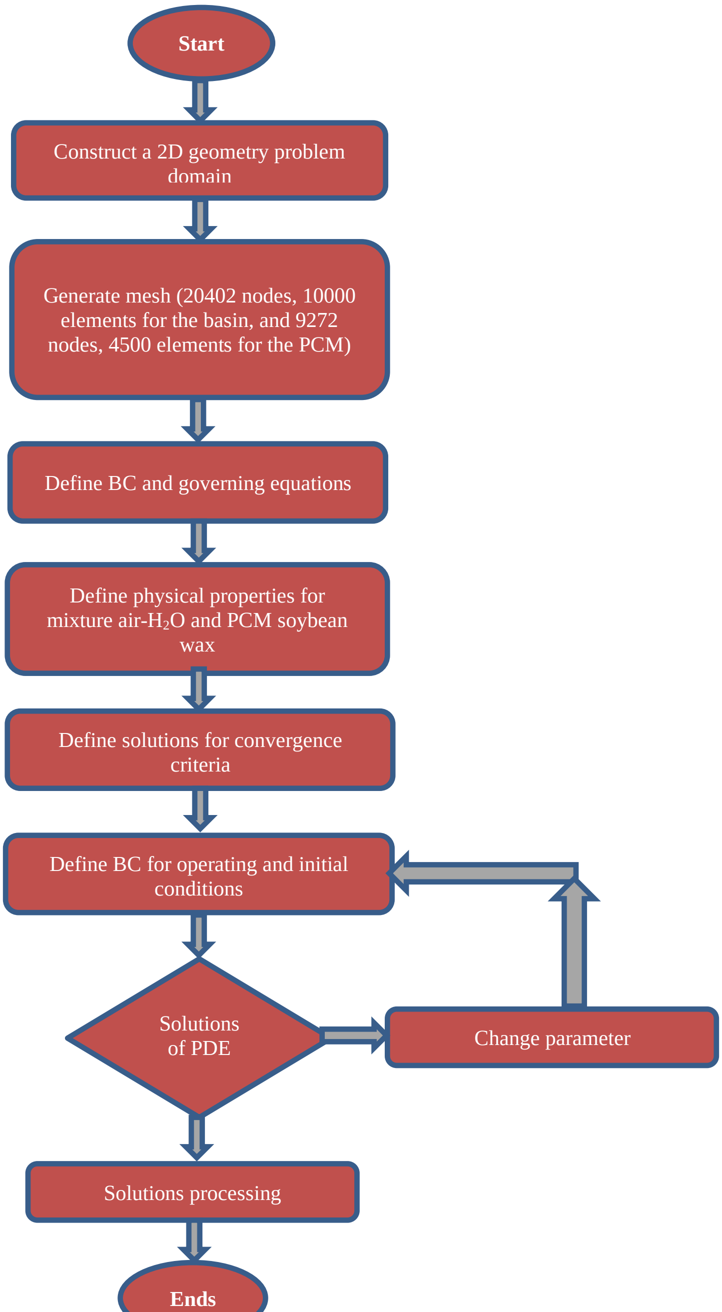


Figure 3. Flowchart research CFD steps.

**The theoretical performance of single slope solar still with PCM.**

The most commonly studied desalination systems are single-slope solar stills. Various techniques, such as numerical methods, computer modeling, periodic and transient analysis, and iterative methods, can be employed to predict the performance of a conventional solar distillation system. Dunkle (Dunkle, 1961) gave the basic internal heat and mass transfer relations, while Tiwari et al. (Tiwari et al., 2003) detailed the process. Using this method, the hourly evaporation from a solar still per square meter is calculated as follows:

$$q_{ew} = 0.0163 h_{cw}(P_w - P_g) \tag{6}$$

Where: $P_w$ = partial vapor pressure at water temperature (N/m$^2$), $P_g$ = partial vapor pressure at glass temperature (N/m$^2$), $h_{cw}$ = convective heat transfer coefficient from water to glass (W/m$^2$ C). The partial vapor pressures at the water and glass temperatures can be obtained from (Belessiotis, Vassilis. Kalogirou, Soteris. Delyannis, 2016):

$$P_W = 100(0.004516 + 0.0007178(T_w) - 2.649x10^{-6}(T_w)^2 + 6.944x10^{-7}(T_w)^3 \quad (7)$$

$$P_g = 100(0.004516 + 0.0007178(T_g) - 2.649x10^{-6}(T_g)^2 + 6.944x10^{-7}(T_g)^3 \quad (8)$$

Where: $T_w$ = Temperature water ($^0$C), $T_g$ = Temperature glass ($^0$C).

The convective heat transfer coefficient ($h_{cw}$) is calculated as (Owolabi et al., 2023):

$$h_{cw} = 0.884\left[(T_w - T_g) + \frac{P_w - P_g}{268900 - P_w} xT_w\right]^{1/3} \quad (9)$$

The numerical values of C and n for different cases are shown in Table 4.

Table 4. Numerical values *C* and *n* (G.N.Tiwari & Lovedeep Sahota, n.d.).

| **Direction of heat flow** | ***C*** | ***n*** |
|---|---|---|
| Upward (hot surface facing upward) | 0.54 | 1/4 |
| Downward (hot surface facing downward) | 0.27 | 1/4 |

The hourly distillate output per square meter from a distiller unit ($\dot{m}$) is given by (Belessiotis, Vassilis. Kalogirou, Soteris. Delyannis, 2016):

$$\dot{m} = 3600\frac{q_{ew}}{L_v} \quad (10)$$

Where: $L_v$ = Latent heat vaporization (kJ/kg)

Another form of Dunkle's model is (Rahbar et al., 2015):

$$N_u = 0.075(R_a)^{1/3} \quad (11)$$

Where :

$$R_a = \frac{\rho^2 g\beta C_p H^3 \Delta T}{\mu k} \quad (12)$$

$$T_i = \frac{T_w + T_g}{2} \quad (13)$$

$$H = \frac{H_l + H_r}{2} \quad (14)$$

The properties of humid air in the equations above are derived from the data outlined in Table 2. Two empirical correlations based on the Bulk-motion and Chiltone-Colburn analogy show improved accuracy compared to Dunkle's model. Their empirical correlations are as follows (Shawaqfeh & Farid, 1995):

$N_{ubm} = 0.057Ra^{1/3}$ Bulk-motion model (15)

$N_{ucc} = 0.051Ra^{1/3}$ Chiltone Colburn model (16)

Where $Ra$ is calculated by Eq (12)

## RESULTS AND DISCUSSIONS

### Contour thermal and streamlines.

The depiction of flow and thermal characteristics in a single-slope solar still with the bottom part augmented with phase change material (PCM) is illustrated in Figures 4 to 7. Figure 4 demonstrates the impact of variations in water temperature (Tw) and glass temperature (Tg) on the isotherms and streamlines. At 9 a.m., the data revealed that the temperature isotherm was aligned with the lower right segment of the cavity, indicating that a convection flow pattern was beginning to form. In the upper region of the cavity, the temperature decreases due to the cooler temperature near the upper wall, while the gradient of the isotherms becomes steeper as it approaches the lower wall. This occurs due to heat transfer during the PCM charging process, resulting in thermal contours showing higher temperatures at the top of the PCM compared to the bottom part. In this region, conductive heat transfer is predominant because the PCM is heated from top to bottom, and the thickness is relatively large.

At noon, the water temperature (Tw) increases, and the isotherms throughout the cavity become predominantly curved, indicating a significant enhancement in the convection process. Similarly, the iso-concentrations display this behavior. As the water temperature (Tw) increases, the vapor gradients near the heated wall become more pronounced. With rising water temperature, buoyancy forces become stronger and dominate the streamlined flow forming three relatively dense convective cells. This leads to improved heat transfer. In this section charging process, the thermal contour of the PCM shows a more uniform distribution, indicating that the PCM is melting but remains in a mushy state as shown in Figure 5. By 3 PM, the temperature and concentration iso-contours still have the same structure. The thermal contour reveals a convection basin with streamlined flow forming three convective cells with relatively wide cavities, as illustrated in Figure 6. In this section, the thermal contour indicates that the PCM is evenly distributed and melting, suggesting that the PCM is beginning to discharge.  At 6 PM, the PCM discharge process was still ongoing, resulting in convective thermal patterns in the single slope solar still. The flow continued to form three convective cells, but the cavities were becoming wider and thinner. At the bottom, the thermal contour of the PCM is uniform, indicating the ongoing discharge process where the PCM has begun to revert to its solid form. This phase occurs when the sunset is depicted in Figure 7.

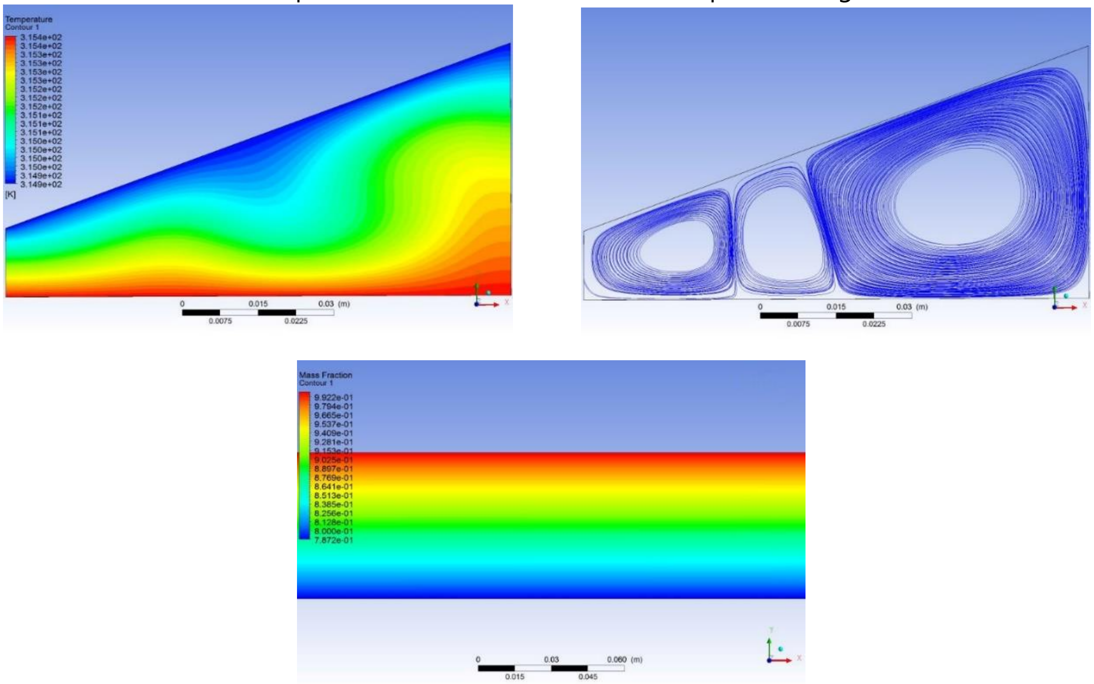

Figure 4. Temperature contours and streamlines of S4 and PCM at 9 AM

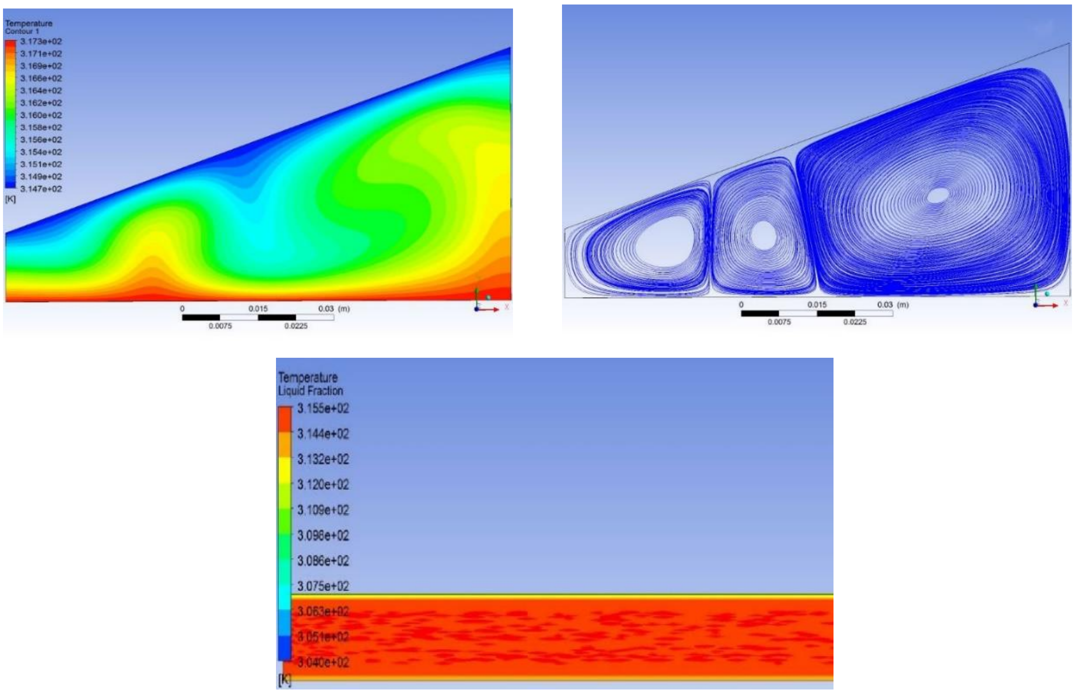


Figure 5. Temperature contours and streamlines of S4 and PCM at 12 AM

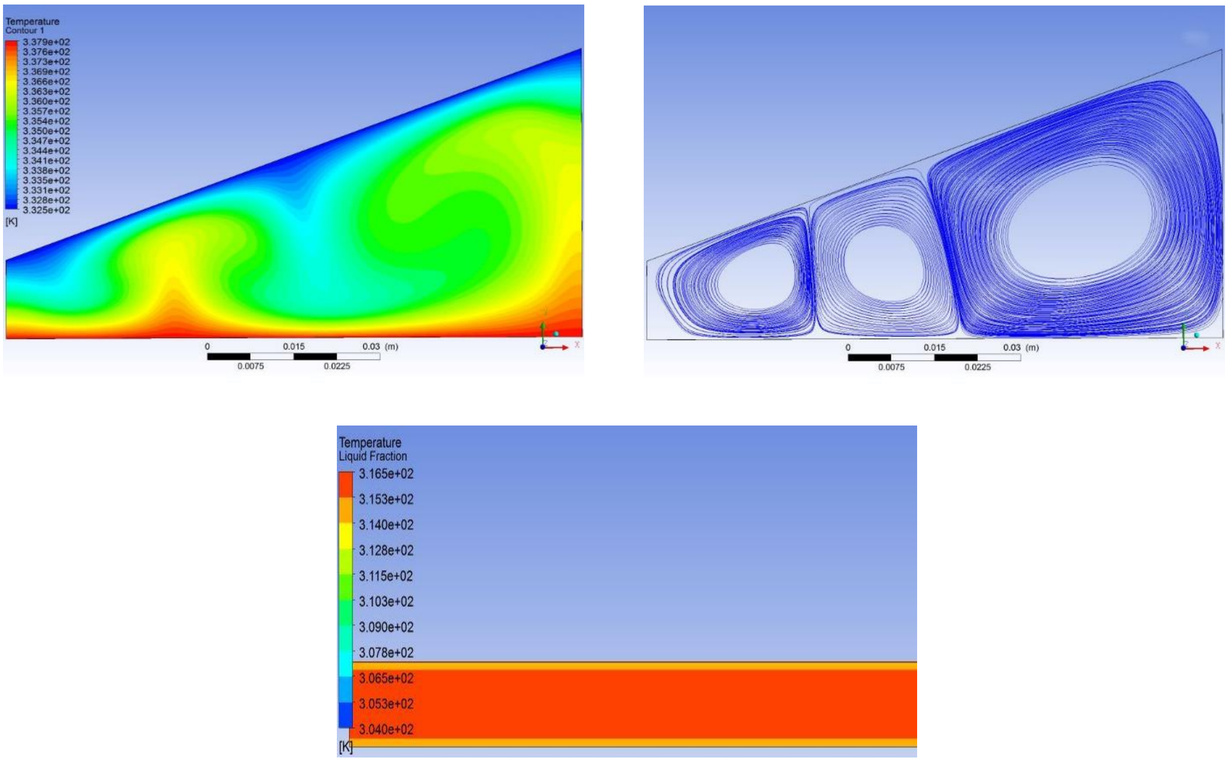


Figure 6. Temperature contours and streamlines of S4 and PCM at 3 PM

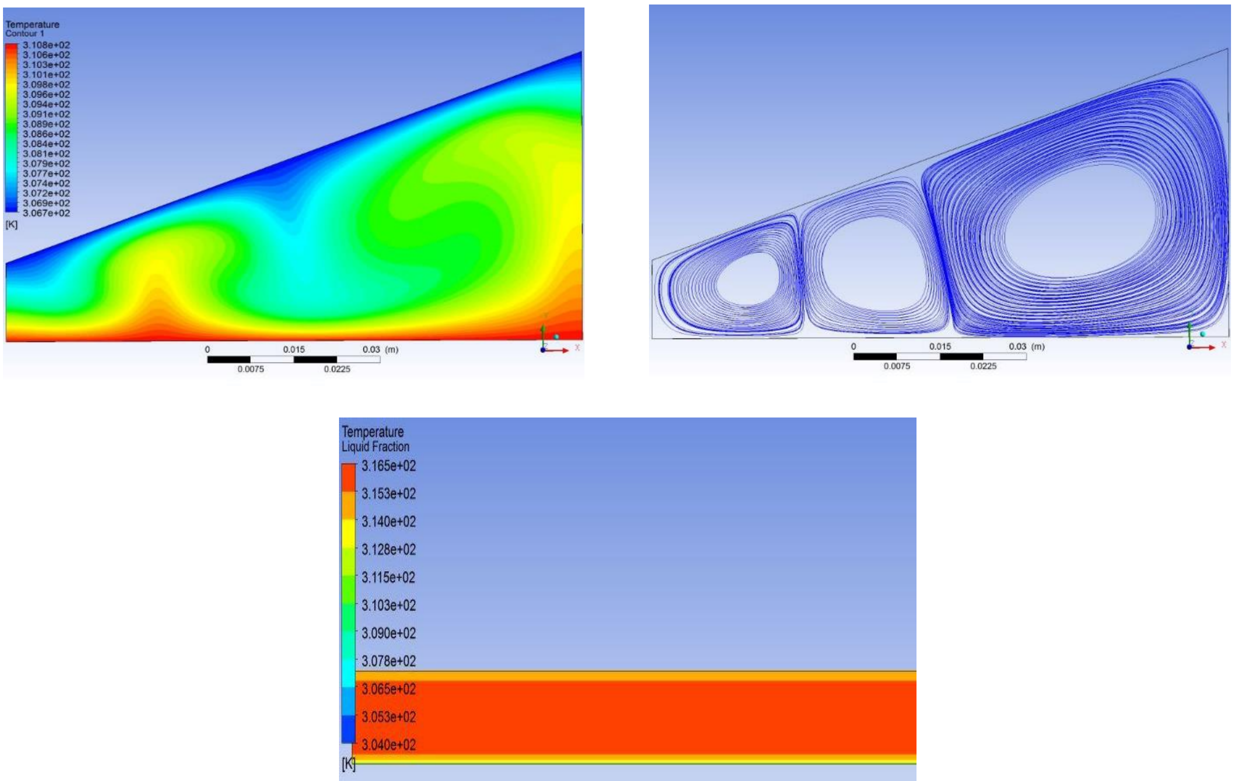


Figure 7. Temperature contours and streamlines of S4 and PCM at 6 PM

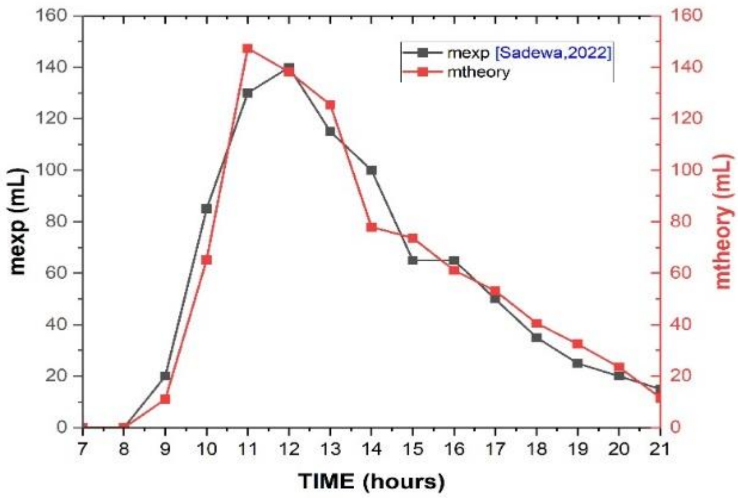


Figure 8. Productivity theory-experiment

**The productivity of single slope solar still with PCM.**

Using equations (6) to (10), the hourly productivity of distilled water shows good agreement between theory and experiment, as illustrated in Figure 8. Tables 5 and 6, demonstrate that the predicted water and glass temperatures from both CFD and experimental data are in good agreement. Additionally, the calculation of Nusselt values for the Dunkle, Chiltone-Colburn, and Bulk-motion models reveals that the differences between these values are minimal.

Table 5. Thermal conditions proposed model with experiment data.

| Time (Hours) | Temperature | | Dunkle's Model | Bulk-motion model | Chiltone-Colburn Model |
|---|---|---|---|---|---|
| | Tw(K) | Tg(K) | $N_u$ | $N_{ubm}$ | $N_{ucc}$ |
| 9 AM | 315.4 | 314.9 | 2.31 | 1.76 | 1.57 |
| 12 AM | 333.8 | 328.5 | 23.33 | 17.73 | 15.86 |
| 3 PM | 323.6 | 319.6 | 18.13 | 13.78 | 12.33 |
| 6 PM | 310.8 | 307.7 | 14.61 | 11.10 | 9.94 |

Table 6. Thermal conditions were used to validate the CFD code and proposed model.

| Time (Hours) | Temperature (Simulated) | | Dunkle's Model | Bulk-motion model | Chiltone-Colburn Model |
|---|---|---|---|---|---|
| | Tw(K) | Tg(K) | $N_u$ | $N_{ubm}$ | $N_{ucc}$ |
| 9 AM | 315.4 | 314.9 | 2.31 | 1.76 | 1.57 |
| 12 AM | 317.3 | 314.7 | 24.45 | 18.58 | 16.63 |
| 3 PM | 337.9 | 332.5 | 17.39 | 13.22 | 11.83 |
| 6 PM | 310.8 | 306.7 | 14.64 | 11.12 | 9.95 |

## CONCLUSIONS

The natural convection within a single-slope solar still, which contains an air-vapor mixture and experiences temperature differences between seawater and the glass wall, has been analyzed numerically. The key conclusions from the results are:

1. The differences in water and glass temperatures significantly affect the flow behavior of the air-$H_2O$ mixture, including streamlines and iso-temperature patterns. Higher water temperatures change the streamlines, with buoyancy forces becoming stronger and dominating the flow, resulting in the formation of three relatively dense convective cells.

2. As the water temperature (Tw) rises, both the size and number of vortices in the streamlines increase.
3. Increasing water temperature (Tw) causes buoyancy forces to surpass viscous forces, leading to thicker thermal and solutal boundary layers.
4. At noon, it was observed that the phase change material (PCM) had melted and turned fully liquid in the afternoon.
5. The CFD model was developed using Fluent to simulate a single-slope solar still incorporating PCM. The model calculates the distillate yield over a full day, considering steady boundary conditions for temperature at the top and bottom surfaces. Additionally, an illustrative simulation showcases the model's capability to capture temperature and streamline contours accurately. This tool proves invaluable for exploring various configurations and optimizing the distiller design to achieve maximum yield.

Recommendations for future work are to research numerically and experimentally by varying the position of the PCM on a single slope solar still placed between seawater and not under the basin.

## REFERENCES

Alwan, N. T., Majeed, M. H., Khudhur, I. M., Shcheklein, S. E., Ali, O. M., Yaqoob, S. J., & Alayi, R. (2022). Assessment of the performance of solar water heater: an experimental and theoretical investigation. *International Journal of Low-Carbon Technologies*, *17*(April), 528–539. https://doi.org/10.1093/ijlct/ctac032

Bansal, K., Kumar, R., Krishna, S., Kumar, P., & Sharma, A. (2022). Materials Today : Proceedings Validation and CFD modeling of solar still with nanoparticle coating on absorber plate. *Materials Today: Proceedings*, *63*, 673–679. https://doi.org/10.1016/j.matpr.2022.04.744

Belessiotis, Vassilis. Kalogirou, Soteris. Delyannis, E. (2016). *Thermal Solar Desalination Thermal Solar Methods and Systems*. Joe Hayton Elsevier. https://doi.org/10.1016/B978-0-12-809656-7.00007-6

Cheng, W. L., Huo, Y. K., & Nian, Y. Le. (2019). Performance of solar still using shape-stabilized PCM: Experimental and theoretical investigation. *Desalination*, *455*(January), 89–99. https://doi.org/10.1016/j.desal.2019.01.007

Clark, J. A. (1990). The steady-state performance of a solar still. *Solar Energy*, *44*(1), 43–49. https://doi.org/10.1016/0038-092X(90)90025-8

Dunkle, R. (1961). Solar water distillation: the roof type still and the multiple effect diffusor. *Int. Dev. in Heat Transfer*, *V*, 9. https://doi.org/2158901

El-Sebaii, A. A., Al-Ghamdi, A. A., Al-Hazmi, F. S., & Faidah, A. S. (2009). Thermal performance of a single basin solar still with PCM as a storage medium. *Applied Energy*, *86*(7–8), 1187–1195. https://doi.org/10.1016/j.apenergy.2008.10.014

G.N.Tiwari & Lovedeep Sahota. (n.d.). *Advanced Solar-Distillation Systems*. Springer.

Ghougali, M., Kabeel, A. E., El, M., Attia, H., Elazab, M. A., & Abdelgaied, M. (2024). Optimal orientation of efficacy metal fins to enhanced freshwater generation in solar distillers: An experimtental study. *Desalination and Water Treatment*, *319*(April), 100479. https://doi.org/10.1016/j.dwt.2024.100479

Gnanavel, C., Saravanan, R., & Chandrasekaran, M. (2021). Materials Today : Proceedings CFD analysis of solar still with PCM. *Materials Today: Proceedings*, *37*, 694–700. https://doi.org/10.1016/j.matpr.2020.05.638

Jahanpanah, M., Sadatinejad, S. J., Kasaeian, A., Jahangir, M. H., & Sarrafha, H. (2021). Experimental investigation of the effects of low-temperature phase change material on single-slope solar still. *Desalination*, *499*(October 2020), 114799. https://doi.org/10.1016/j.desal.2020.114799

Jeon, J., Hun, J., Wi, S., Yang, S., Sik, Y., & Kim, S. (2019). Latent heat storage biocomposites of phase change material-biochar as feasible eco-friendly building materials. *Environmental Research*, *172*(December 2018), 637–648. https://doi.org/10.1016/j.envres.2019.01.058

Kabeel, A. E., & El-Said, E. M. S. (2015). Water production for irrigation and drinking needs in remote arid communities using closed-system greenhouse: A review. *Engineering Science and Technology, an International Journal*, *18*(2), 294–301. https://doi.org/10.1016/j.jestch.2014.12.003

Ouled Saad, F., Mankai, S., Madiouli, J., Chemkhi, S., Shigidi, I., & Khan, M. I. (2024). Effect of phase change materials melting temperature on improving single slope solar still productivity. *Journal of Energy Storage*, *97*(PB), 112927. https://doi.org/10.1016/j.est.2024.112927

Owolabi, L., Chintua, C., Kareem, M. W., Arogundade, A. I., Irshad, K., Islam, S., Oladosu, K. O., & Elfaghi, A. M. (2023). Experimental investigation of double slope solar still integrated with PCM nanoadditives microencapsulated thermal energy storage. *Desalination*, *553*(August 2022), 116477. https://doi.org/10.1016/j.desal.2023.116477

Prakash, O., Ahmad, A., Kumar, A., Mozammil Hasnain, S. M., & Kumar, G. (2022). Comprehensive analysis of design software application in solar distillation units. *Materials Science for Energy Technologies*, *5*, 171–180. https://doi.org/10.1016/j.mset.2022.01.005

Rahbar, N., Esfahani, J. A., & Fotouhi-Bafghi, E. (2015). Estimation of convective heat transfer coefficient and water-productivity in a tubular solar still - CFD simulation and theoretical analysis. *Solar Energy*, *113*, 313–323. https://doi.org/10.1016/j.solener.2014.12.032

Rajaseenivasan, T., & Srithar, K. (2016). Performance investigation on solar still with circular and square fins in basin with CO2 mitigation and economic analysis. *DES*, *380*, 66–74. https://doi.org/10.1016/j.desal.2015.11.025

Sadewa, D. M., Septiyanto, M. D., Yaningsih, I., Budiana, E. P., Hadi, S., & Prasetyo, A. (2024). *Performance Testing of Single Slope Solar Still by Using Soybean Wax as PCM BT - Proceedings of the 9th International Conference and Exhibition on Sustainable Energy and Advanced Materials* (M. A. Salim, N. S. Khashi'ie, K. W. Chew, & C. Photong (eds.); pp. 307–311). Springer Nature Singapore.

Saleem, K. B., Ghachem, K., Koufi, L., & Kolsi, L. (2021). Analysis of Double-diffusive natural convection in a solar distiller embedded with PCM and cooled with external water stream. *Journal of the Taiwan Institute of Chemical Engineers*, *126*, 67–79. https://doi.org/10.1016/j.jtice.2021.06.042

Saleem, K. B., Koufi, L., Alshara, A. K., & Kolsi, L. (2020). Double-diffusive natural convection in a solar distiller with external fluid stream cooling. *International Journal of Mechanical Sciences*, *181*(May). https://doi.org/10.1016/j.ijmecsci.2020.105728

Sarhaddi, F., Farshchi Tabrizi, F., Aghaei Zoori, H., & Mousavi, S. A. H. S. (2017). Comparative study of two weir type cascade solar stills with and without PCM storage using energy and exergy analysis. *Energy Conversion and Management*, *133*, 97–109. https://doi.org/10.1016/j.enconman.2016.11.044

Shalaby, S. M., El-Bialy, E., & El-Sebaii, A. A. (2016). An experimental investigation of a v-corrugated absorber single-basin solar still using PCM. *Desalination*, *398*, 247–255. https://doi.org/10.1016/j.desal.2016.07.042

Shawaqfeh, A. T., & Farid, M. M. (1995). New development in the theory of heat and mass transfer in solar stills. *Solar Energy*, *55*(6), 527–535. https://doi.org/10.1016/0038-092X(95)00069-4

Singh, V. K., & Kumar, D. (2024). An experimental investigation and thermo-economic performance analysis of solar desalination system by using nano-enhanced PCM. *Materials Today Sustainability*, *27*(June), 100884. https://doi.org/10.1016/j.mtsust.2024.100884

Taylor, P., Rahbar, N., & Esfahani, J. A. (2012). *Desalination and Water Treatment Estimation of convective heat transfer coefficient in a single-slope solar still: a numerical study*. *January 2014*, 37–41. https://doi.org/10.1080/19443994.2012.720442

Tiwari, G. N., Singh, H. N., & Tripathi, R. (2003). Present status of solar distillation. *Solar Energy*, *75*(5), 367–373. https://doi.org/https://doi.org/10.1016/j.solener.2003.07.005

Trisnadewi, T., Kusrini, E., Marta, D., & Putra, N. (2021). Experimental analysis of natural wax as phase change material by thermal cycling test using thermoelectric system. *Journal of Energy Storage*, *40*(May), 102703. https://doi.org/10.1016/j.est.2021.102703

Velmurugan, V., Gopalakrishnan, M., Raghu, R., & Srithar, K. (2008). *Single basin solar still with fin for enhancing productivity*. *49*, 2602–2608. https://doi.org/10.1016/j.enconman.2008.05.010

Yoo, J., Chang, S. J., Wi, S., & Kim, S. (2019). Chemosphere Spent coffee grounds as supporting materials to produce bio- composite PCM with natural waxes. *Chemosphere*, *235*, 626–635. https://doi.org/10.1016/j.chemosphere.2019.06.195